Total Cross Section for $p+p \rightarrow p+p+\pi^0$ near Threshold Measured with the Indiana Cooler

H. O. Meyer, M. A. Ross, R. E. Pollock, A. Berdoz, F. Dohrmann, J. E. Goodwin, M. G. Minty, H. Nann, P. V. Pancella, S. F. Pate, B. v. Przewoski, T. Rinckel, and F. Sperisen

Department of Physics and Indiana University Cyclotron Facility, Indiana University, Bloomington, Indiana 47405

(Received 24 July 1990; revised manuscript received 10 October 1990)

The total cross section for the reaction $pp \rightarrow pp\pi^0$ was measured at nine center-of-mass energies from 1.5 to 23 MeV above threshold. The experiment was carried out with the Indiana Cooler, a recently constructed storage ring. The experimental advantages of an electron-cooled proton beam were utilized. The data cover an energy range where only the lowest possible angular momentum state contributes in the exit channel. The measured energy dependence of the total cross section is not compatible with that predicted by models of s-wave pion production and rescattering.

PACS numbers: 25.10.+s, 13.75.Cs, 21.30.+y, 29.25.Fb

Meson-exchange models of the nucleon-nucleon (NN) interaction above the pion threshold rely on detailed information about the strongly coupled inelastic channels which must be treated coherently with the elastic interaction. Information on pion production in the NN system is also required in models of pion production or absorption in nuclei. Customarily, the partial waves in the exit channel of $NN \rightarrow NN\pi$ reactions are labeled by Ll, where L is the angular momentum of the nucleon pair and l is the angular momentum of the pion with respect to the nucleon pair.[1] Within 100 MeV of threshold, because of the short range of the interaction, only Ss, Sp, Ps, and Pp final states contribute significantly; within 25 MeV the Ss configuration should dominate. In addition, the Sp final state is forbidden in the $pp \rightarrow pp\pi^0$ reaction.

In the $pp \rightarrow pp\pi^0$ reaction, the normally dominant pion production via an intermediate ΔN system is suppressed, since the N and the Δ cannot be in a relative S state. The rescattering contribution is also small because the dominant isovector part of low-energy πN scattering cannot contribute. Thus, near threshold, the $pp \rightarrow pp\pi^0$ reaction is dominated by the direct-production Born term.[2] The energy dependence of the cross section is customarily expressed in terms of η, the largest possible center-of-mass pion momentum (with nucleons at rest relative to each other) divided by the pion mass. Based on phase-space arguments, the assumption of $\eta \ll 1$, and a simple treatment of the final-state interaction, one expects[3] for the total cross section

$$\sigma_{\text{tot}} = B_0\eta^2 + B_1\eta^6 + B_2\eta^8, \quad (1)$$

where the three terms correspond to the Ss, Ps, and Pp final states, respectively.

Sufficiently close to threshold for $pp \rightarrow pp\pi^0$, only the Ss exit channel contributes, with the two nucleons in a $^1S_0$ state. In this case, the entrance channel is limited to a single partial wave ($^3P_0$). This should greatly simplify the theoretical interpretation of the data. The experiment described here is the first to cover this energy range. Previous experiments were hampered by the fact that the cross section (due to the suppressed resonant production) is small and competes with background caused by nuclei other than hydrogen in the path of the beam. Because of the properties of the novel experimental environment described below, it becomes feasible to measure the four-momenta of both outgoing protons, making it possible to completely reconstruct the three-body final state.

The measurement was carried out with the Indiana Cooler,[4] a newly constructed storage ring equipped with an intense, comoving electron beam for phase-space cooling[5] of the stored proton beam; it is the first nuclear physics experiment carried out with such a device. The experiment, illustrating well the potential of the new technology, uses synchrotron acceleration, which gives the Indiana University Cyclotron Facility access to the $NN\pi$ threshold, and benefits from the small-interaction-energy spread, the low background due to the windowless target, the accessibility of small reaction angles, and the observability of low-energy recoils.

In the hexagonal lattice of the storage ring[4] three straight sections contain equipment for injection, electron cooling, and beam manipulation, while the others are provided for experiments. Figure 1 shows the internal target mounted in the center of the section preceding the electron-cooling device. A hydrogen gas jet, emerging from 0.11-mm-diam nozzle (N) cooled to 40 K, crosses the stored proton beam. Half of the gas flow (typically 6×10^{19} molecules/s) is pumped away through a catcher (C) opposite the jet. The remainder of the gas is removed in a three-stage differential pumping arrangement (1–3, in Fig. 1) along the beam axis. This resulted in a pure hydrogen target of $(2\text{–}5)\times10^{15}$-atoms/cm^2 thickness. The width of the jet at beam height was 3 mm FWHM; about 80% of the target thickness was concentrated within ± 1 cm of the jet. At the target, the unobstructed area through which the beam passed was

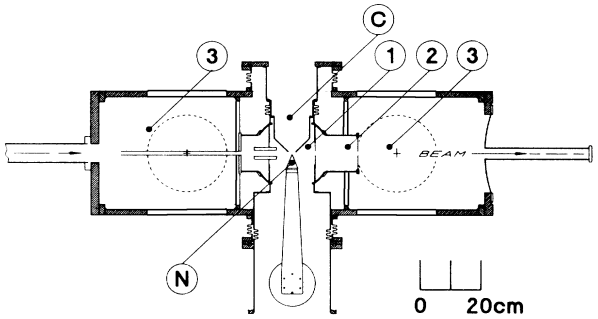

FIG. 1. The target chamber with the internal gas-jet target with nozzle (N) and catcher (C). The numbers indicate the three stages for differential pumping. Also shown is the thin exit foil on the downstream end.

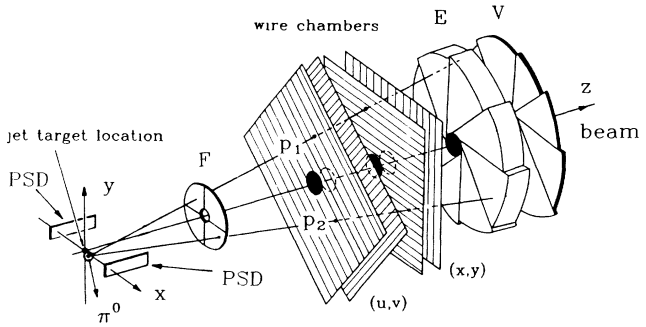

FIG. 2. Schematic view of the detector setup. Shown are the scintillator arrays F, E, and V and the two wire-chamber pairs needed for the unambiguous determination of two coincident particle tracks. Two position-sensitive silicon detectors (PSD) are used to observe the recoil in $p+p$ elastic scattering.

12 mm high and 24 mm wide. The pumping apertures on the downstream side were holes in 24-μm-thick aluminum foils and the end of the target box consisted of a 127-μm-thick steel foil. This minimizes the amount of material the exiting charged particles have to traverse.

The detector arrangement downstream of the target chamber has cylindrical symmetry around the beam axis (see Fig. 2). A 1.5-mm-thick scintillator (F), segmented into quadrants, is followed by two pairs of orthogonal wire planes, and by a 102-mm-thick (E) and a 6.4-mm-thick (V) scintillator, both segmented into octants. The wire chambers have a wire separation of 6.4 mm and are of a special design,[6] which features a central hole for the beam pipe. The wire chambers determine the direction of outgoing charged particles. Near threshold, the laboratory angle of protons from the $pp \rightarrow pp\pi^0$ reaction is limited: The detector was built to completely cover this angular region, with the exception of the central hole. As the bombarding energy was changed, the positions of the detector elements were adjusted in order to accommodate corresponding changes in the kinematically allowed cone. In addition, for the measurements above 290 MeV, the jet target was moved from the middle position in the target box (Fig. 1) to a position closer to the exit foil. The thickness of the E detector was chosen to stop protons resulting from pion production (up to 120 MeV). The trigger for $pp\pi^0$ events was a coincidence between E and F, but no pulse in V; in addition, more than one segment of the E detector was required to fire, signaling at least two observed particles.

Data were acquired in so-called cycles. Each cycle consisted of injection of 45-MeV protons via dissociation of a 90-MeV incident H_2^+ beam on a thin carbon stripper foil (≈ 2 s), acceleration to the final energy (≈ 4 s), data acquisition with the internal target while cooling (≈ 10 s), and restoration of initial conditions (≈ 4 s). Stored beam currents ranged from 5 to 25 μA, resulting in a typical average luminosity of 5×10^{28} cm^{-2}s^{-1}. During a total time for production runs of 110 h, an integrated luminosity of about 16 nb^{-1} was achieved.

Charged particles were identified as protons by a condition on the relation between the time of flight from the F to the E detector and the energy deposited in the E detector. From the latter and the direction obtained from the wire chambers, the mass m_3 of the unobserved particle was reconstructed: Figure 3 shows a clean peak at the π^0 mass. The area under this peak determines the number N_π of observed $pp\pi^0$ events. The detector performance was compared with a Monte Carlo simulation and good agreement was found. Using this comparison, the bombarding energy was determined with a precision of ± 200 keV from the strongly energy-dependent maximum laboratory angle of the $pp\pi^0$ protons. The fraction of $pp\pi^0$ events that are not seen due to the dead zone in the center of the detector was extrapolated from the measured distribution of proton scattering angles. The shape of the extrapolating function was based on the Monte Carlo simulation. The effective range expansion was used to include in the simulation the final-state interaction between the two nucleons.

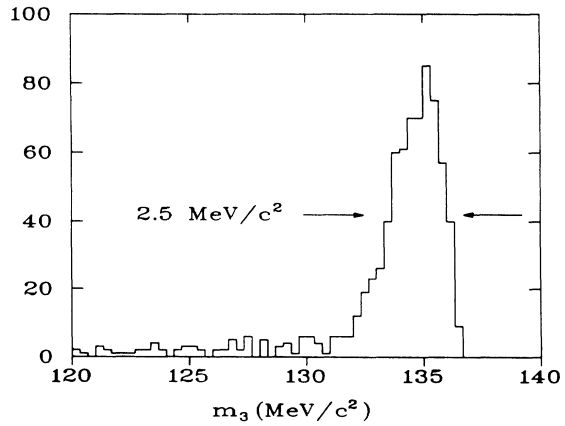

FIG. 3. Histogram of the reconstructed mass m_3 of the unobserved particle. The bombarding energy in this case was 282.5 MeV.

The absolute normalization of the cross section was obtained from $p+p$ elastic scattering, observed concurrently with pion production. Elastic-scattering events triggered a coincidence between all three scintillator planes. At the most forward angles, it was found that a large fraction of the detected protons were beam protons outside the ring acceptance scattering from material close to the beam. In order to reject such events, low-energy recoil protons from $p+p$ elastic scattering were observed in coincidence by two 7-mm by 45-mm position-sensitive silicon detectors (PSD in Fig. 2) mounted 11 cm from the beam on either side of the jet with the position-sensitive direction parallel to the beam axis. Practically all coincidences between a forward proton and a recoil in the silicon detectors satisfied the kinematics of $p+p$ elastic scattering. These events were counted simultaneously with $pp\pi^0$ events. From the published $p+p$ elastic-scattering cross section[7] in the corresponding angle and energy interval, the integrated luminosity was deduced. From the position of the recoils in the silicon detector and the angle of the forward protons, the distribution of the scattering centers, and thus the profile of the gas jet and the contribution of the uniform gas density outside the jet region, was determined.

The final results are listed in Table I. The total cross section $\sigma_{\rm tot}$ follows from the observed number of pions N_π, the absolute integrated luminosity L deduced from $p+p$ elastic scattering, and a correction factor g. This factor is mainly due to a 15%–40% loss of $pp\pi^0$ events due to the dead zone of the central hole; smaller contributions include the measured wire-chamber efficiency (3%–7%), and the scintillator efficiency (1%–4%). The quoted errors contain the contribution from counting statistics as well as an estimated uncertainty in the luminosity and the correction factor g. An overall normalization error of 5% owing to an estimated uncertainty of the $p+p$ elastic cross section[7] is not included.

TABLE I. The laboratory bombarding energy $T_{\rm lab}$ (known to ± 200 keV), the parameter η (see text), the number N_π of $pp\pi^0$ events collected, the applied correction factor g (discussed in the text), the integrated luminosity L deduced from $p+p$ scattering, and the result for the total cross section $\sigma_{\rm tot}$. The quoted error includes statistics and systematic contributions but does not contain the uncertainty of the $p+p$ scattering cross section which would add an estimated 5% error to the overall normalization.

$T_{\rm lab}$ (MeV)	η	N_π	g	L (nb^{-1})	$\sigma_{\rm tot}$ (μb)
282.5	0.136	801	1.69	4.48	0.30 ± 0.02
283.9	0.166	1027	1.43	2.94	0.50 ± 0.04
286.5	0.211	3461	1.21	4.49	0.93 ± 0.06
289.2	0.250	1521	1.18	1.24	1.44 ± 0.09
292.4	0.289	968	1.31	0.794	1.60 ± 0.15
300.5	0.372	1186	1.22	0.450	3.22 ± 0.22
309.2	0.445	1907	1.20	0.506	4.52 ± 0.30
316.6	0.500	2231	1.24	0.451	6.15 ± 0.43
325.0	0.557	573	1.26	0.090	8.05 ± 0.67

The experimental procedure was checked by carrying out a number of measurements at the same energy, but separated in time, or with a diffuse target instead of a jet, or with different detector positions. These runs yielded consistent results and demonstrated reproducibility and the validity of the methods used to obtain the luminosity and correct for geometric losses.

In Fig. 4 our results for the total cross section $\sigma_{\rm tot}$, divided by η^2, are shown versus η as solid dots, together with previous measurements.[8-11] Using Eq. (1), previously published three-parameter fits (dashed line[9] and dot-dashed line[11]) yield the coefficients $B_0 = 32$ μb and $B_0 = 15.6$ μb for the contribution of the lowest angular momentum state. These should be compared to theoretical values[2,12] between 11 and 18 μb. Such an analysis assumes that the cross section for small enough η is indeed proportional to η^2. Since our data seem to contradict such a dependence, we have reevaluated the energy dependence due to phase space and the final-state interaction between the two S-state protons. Multiplying the phase-space element [e.g., Eq. (6), Ref. 13] by the final-state interaction weight,[14] based on a charged effective range expansion, and integrating over the remaining kinematical variable, we have obtained the Ss cross section as a function of η (scaled by an arbitrary factor). The result is shown as a dotted curve in Fig. 4. The decrease of $\sigma_{\rm tot}/\eta^2$ below $\eta \sim 0.25$ predicted by this calculation, which is clearly supported by the present

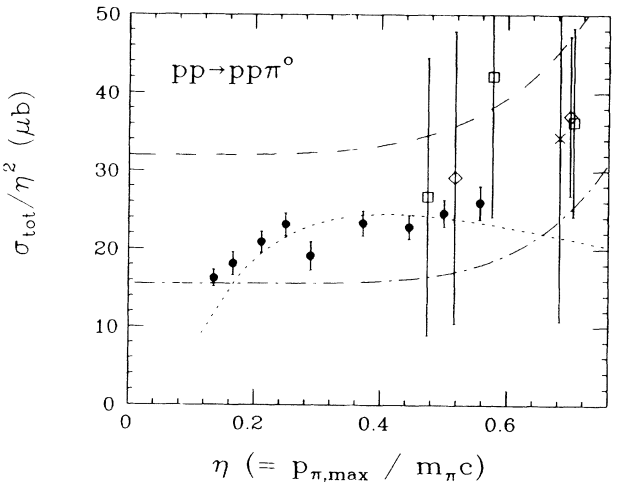

FIG. 4. The total cross section divided by η^2 for $pp \rightarrow pp\pi^0$ vs η. The present data are shown as solid dots; their errors do not include a 5% uncertainty of the overall normalization. Other data are from Ref. 8 (cross), Ref. 9 (squares), and Ref. 11 (diamonds). The dashed and dot-dashed curves are previous three-parameter fits using Eq. (1) (see text). The dotted curve shows the energy dependence of the Ss cross section due to phase space and the final-state interaction between the two protons.

data, is due to the interaction between the two outgoing protons. We conclude that the assumptions previously made[2] in deriving the energy dependence are not valid at small η and that a detailed study of σ_{tot} at small η is likely to yield information on the short-range part of the NN interaction and is certainly needed in order to compare the data with calculations of the transition matrix element. Such calculations should be facilitated by the fact that the matrix element is dominated by the Born term and that only one partial wave contributes. Finally, we note that the datum at $\eta=0.289$, which is significantly low, coincides with the threshold of the process $pp \rightarrow pn\pi^+$. Further experimental study of the $pp \rightarrow pp\pi^0$ cross section near this energy is planned.

We are grateful to the operating team of the new machine, in particular to D. Friesel, T. Sloan, and V. Derenchuk for their tireless effort in bringing the new machine on line, and to M. Macfarlane for help on theoretical issues. J. Doskow has provided technical expertise in constructing the internal target and H. Rohdjess has contributed one of the figures. This work has been supported in part by the Deutscher Akademischer Austauschdienst and by the U.S. National Science Foundation under Grant No. NSF PHY 87-14406.

[1]A. H. Rosenfeld, Phys. Rev. **96**, 139 (1954).

[2]D. S. Koltun and A. Reitan, Phys. Rev. **141**, 1413 (1966).

[3]M. Gell-Mann and K. M. Watson, Annu. Rev. Nucl. Sci. **4**, 219 (1954).

[4]R. E. Pollock, in *Proceedings of the IEEE Particle Accelerator Conference, Chicago, 1989,* edited by F. Bennett and J. Kopta (IEEE, New York, 1989), p. 17.

[5]F. T. Cole and F. E. Mills, Annu. Rev. Nucl. Part. Sci. **31**, 295 (1981), and references therein.

[6]K. Solberg, A. Eads, J. Goodwin, P. Pancella, H. O. Meyer, T. Rinckel, and A. Ross, Nucl. Instrum. Methods Phys. Res., Sect. A **281**, 283 (1989).

[7]R. A. Arndt, L. D. Roper, R. A. Bryan, R. B. Clark, B. J. VerWest, and P. Signell, Phys. Rev. D **28**, 97 (1983), and the database SAID mentioned therein.

[8]R. A. Stallwood, R. B. Sutton, P. H. Fields, J. G. Fox, and J. A. Kane, Phys. Rev. **109**, 1716 (1958).

[9]A. F. Dunaitsev and Yu.D. Prokoshkin, Zh. Eksp. Teor. Fiz. **36**, 1656 (1959) [Sov. Phys. JETP **9**, 1179 (1959)].

[10]F. Shimizu, Y. Kubota, H. Koiso, F. Sai, S. Sakamoto, and S. S. Yamamoto, Nucl. Phys. **A386**, 571 (1982).

[11]S. Stanislaus, D. Horvath, D. F. Measday, and A. J. Noble, Phys. Rev. C **41**, R1913 (1990).

[12]V. P. Efrosinin, D. A. Zaikin, and I. I. Osipchuk, Z. Phys. A **322**, 573 (1985).

[13]R. Handler, Phys. Rev. **138**, B1230 (1965).

[14]B. J. Morton *et al.*, Phys. Rev. **169**, 825 (1968).